

Supplementary Material

Mosaic RBD nanoparticles protect against multiple sarbecovirus challenges in animal models

Short title: Mosaic-8 RBD nanoparticle protects from SARS-2 and SARS-1 challenges; homotypic SARS-2 nanoparticle protects only from SARS-2

Alexander A. Cohen^{1†}, Neeltje van Doremalen^{2†}, Allison J. Greaney³, Hanne Andersen⁴, Ankur Sharma⁴, Tyler N. Starr³, Jennifer R. Keeffe¹, Chengcheng Fan¹, Jonathan E. Schulz², Priyanthi N.P. Gnanapragasam¹, Leesa M. Kakutani¹, Anthony P. West, Jr.¹, Greg Saturday², Yu E. Lee^{1‡}, Han Gao¹, Claudia A. Jette¹, Mark G. Lewis⁴, Tiong K. Tan⁵, Alain R. Townsend^{5,6}, Jesse D. Bloom⁷, Vincent J. Munster², Pamela J. Bjorkman^{1*}

¹Division of Biology and Biological Engineering, California Institute of Technology, Pasadena, CA 91125, USA.

²Laboratory of Virology, National Institute of Allergy and Infectious Diseases, National Institutes of Health, Hamilton, MT 59840, USA.

³Basic Sciences Division and Computational Biology Program, Fred Hutchinson Cancer Research Center, Seattle, WA 98109, USA; Department of Genome Sciences & Medical Scientist Training Program, University of Washington, Seattle, WA 98195, USA.

⁴BIOQUAL, Rockville, MD, USA.

⁵MRC Human Immunology Unit, MRC Weatherall Institute of Molecular Medicine, John Radcliffe Hospital, University of Oxford, Oxford OX3 9DS, UK.

⁶Centre for Translational Immunology, Chinese Academy of Medical Sciences, Oxford Institute, University of Oxford, Oxford OX3 9DS, UK.

⁷Basic Sciences Division and Computational Biology Program, Fred Hutchinson Cancer Research Center, Seattle, WA 98109, USA; Howard Hughes Medical Institute, Seattle, WA 98109, USA.

† Co-first authors

‡ Present address: Department of Biology, Stanford University, Stanford, CA 94305, USA

*Corresponding author: email: bjorkman@caltech.edu

MATERIALS AND METHODS

Protein Expression. Mammalian expression vectors encoding the RBDs of SARS-2 Beta (GenBank QUT64557.1), SARS-CoV-2 Wuhan-Hu-1 (GenBank MN985325.1), RaTG13-CoV (GenBank QHR63300), SHC014-CoV (GenBank KC881005), Rs4081-CoV (GenBank KY417143), pangolin17-CoV (GenBank QIA48632), RmYN02-CoV (GSAID EPI_ISL_412977), Rf1-CoV (GenBank DQ412042), W1V1-CoV (GenBank KF367457), Yun11-CoV (GenBank JX993988), BM-4831-CoV (GenBank NC014470), BtkY72-CoV (GenBank KY352407), Khosta-2 CoV(QVN46569.1), RsSTT200-CoV (EPI_ISL_852605), LYRa3 (AHX37569.1) and SARS-CoV S (GenBank AAP13441.1) with an N-terminal human IL-2 or Mu phosphatase signal peptide were constructed as previously described (34, 82). 5 of the 8 RBD genes (SARS-2, RaTG13, pang17, W1V1, and SHC014) used to make mosaic-8gm were altered by site-directed mutagenesis to include a potential N-linked glycosylation site (PNGS) (N at position 484 and T at position 486). Each RBD was expressed to include a C-terminal hexahistidine tag (G-HHHHHH) and SpyTag003 (RGVPHIVMVDAYKRYK) (38) (for coupling to SpyCatcher003-mi3) or only a 15-residue Avi-tag (GLNDIFEAQKIEWHE) followed by a 6xHis tag (for ELISAs). RBDs were purified from transiently-transfected Expi293F cell (Gibco) supernatants by Ni-NTA and size-exclusion chromatography (SEC) as described (82), and RBDs with an introduced PNGS used for making mosaic-8gm RBD-mi3 were compared to their counterpart RBDs by SDS-PAGE to verify addition of extra N-glycans. SEC RBD fractions identified by SDS-PAGE were pooled and stored at 4°C or frozen in liquid nitrogen and stored at -80°C for longer term storage. A soluble SARS-2 trimer with 6P stabilizing mutations (83) was expressed and purified as described (26). Monoclonal human IgGs and human ACE-2 fused to human IgG Fc (hACE2-Fc) was expressed and purified as described (26, 32).

Preparation of RBD-mi3 nanoparticles. SpyCatcher003-mi3 nanoparticles (78) were expressed in BL21 (DE3)-RIPL *E coli* (Agilent) transformed with the pET28a His6-SpyCatcher003-mi3 gene (Addgene) as described (34, 84). Briefly, transformed bacterial cell pellets were lysed in the presence of 2.0 mM PMSF (Sigma). Lysates were spun at 21,000xg for 30 min, filtered with a 0.2 µm filter, and mi3 particles were isolated by Ni-NTA chromatography using a HisTrap™ HP column (GE Healthcare). Eluted particles were concentrated using an Amicon Ultra 15 mL 30K concentrator (MilliporeSigma) and SEC purified using a HiLoad® 16/600 Superdex® 200 (GE Healthcare) column equilibrated with 25 mM Tris-HCl pH 8.0, 150 mM NaCl, 0.02% NaN₃ (TBS). SpyCatcher003-mi3 particles were stored at 4°C for up to 1 month and used for conjugations after 0.2 µm filtering or spinning at 21,000xg for 10 min.

Purified SpyCatcher003-mi3 nanoparticles were incubated with a 2-fold molar excess (RBD to mi3 subunit) of SpyTagged RBD (either a single RBD for homotypic SARS-2 RBD particles or an equimolar mixture of eight RBDs for mosaic particles) overnight at room temperature in TBS. The nanoparticles included the following RBDs: SARS-2 Beta (homotypic RBD-mi3); SARS-2 Beta, RaTG13, SHC014, Rs4081, RmYN02, pang17, Rf1, and W1V1 (mosaic-8b RBD-mi3); and N-glycan modified versions of the clade 1a and 1b RBDs (Wuhan-Hu-1 SARS-2, RaTG13, SHC014, pang17, and W1V1) together with unmodified Rs4081, RmYN02, and Rf1 RBDs (mosaic-8gm RBD-mi3). For mosaic-8 mi3 nanoparticles, equivalent conjugation of each of the eight SpyTagged RBDs was verified as described by SEC and SDS-PAGE analysis of conjugations to make homotypic nanoparticles (34).

Conjugated RBD-mi3 particles were separated from free RBDs by SEC on a Superose 6 10/300 column (GE Healthcare) equilibrated with PBS (20 mM sodium phosphate pH 7.5, 150 mM NaCl) and fractions corresponding to conjugated RBD-mi3 and free RBD were identified by SDS-PAGE.

Concentrations of conjugated mi3 particles were determined using a Bio-Rad Protein Assay and are reported based on RBD content.

RBD-mi3 nanoparticles were evaluated for binding to a human ACE2-Fc construct (32) and to human monoclonal antibodies that recognize known RBD epitopes by ELISA. Duplicate samples of 20 μ L of a 2.5 μ g/mL solution of a purified RBD-mi3 nanoparticle in 0.1 M NaHCO₃ pH 9.8 was coated onto Nunc® MaxiSorp™ 384-well plates (Sigma) and incubated overnight at 4°C. After blocking with 3% bovine serum albumin (BSA) in TBS containing 0.1% Tween 20 (TBS-T) for 1 hr at room temperature, plates were washed with TBS-T, and purified hACE2-Fc or human IgG (50 μ g/mL with 8 4-fold serial dilutions in TBS-T/3% BSA) was added to plates for 3 hr at room temperature. Plates were then washed again for 1 hr at room temperature, and a 1:100,000 dilution of secondary HRP-conjugated goat anti-human IgG (Abcam) was added. SuperSignal™ ELISA Femto Maximum Sensitivity Substrate (ThermoFisher) was added to plates following manufacturer instructions, and plates were read at 425 nm. For the homotypic SARS-2 Beta ELISA shown in fig. S2F, 50 μ L of a 2.5 μ g/mL solution of a purified RBD-mi3 nanoparticle in 0.1 M NaHCO₃ pH 9.8 was coated onto Corning® 96 well plates (Sigma) and incubated overnight at 4°C. After blocking with 3% bovine serum albumin (BSA) in TBS containing 0.1% Tween 20 (TBS-T) for 1 hr at room temperature, plates were washed with TBS-T, and purified hACE2-Fc or human IgG (50 μ g/mL with 8 serial dilutions 4-fold in TBS-T/3% BSA) was added to plates for 3 hr at room temperature. Plates were then washed again for 1 hr at room temperature, and a 1:10,000 dilution of secondary HRP-conjugated goat anti-human IgG (Abcam) was added. 1-step Ultra TMB-ELISA (ThermoFisher) was added to plates following manufacturer instructions, and plates were read at 450 nm.

Prior to shipping for immunization and challenge studies, aliquots of conjugated RBD-mi3 nanoparticles were frozen in liquid nitrogen and then lyophilized (35) in PBS pH 7.4 using a Labconco CentriVap Benchtop Concentrator at -4°C. For immunizations, distilled water was added to rehydrate to a concentration of 1 mg/mL for a working stock, and the solution was gently pipetted and then spun at 20,000 x g for 10 minutes to remove aggregates.

DLS and EM characterizations of RBD-mi3 nanoparticles. DLS was used to evaluate the hydrodynamic radii of conjugated nanoparticles. Lyophilized nanoparticles were rehydrated as described above. Sample sizes of 100 μ L were loaded into a disposable cuvette, and DLS measurements were performed on a DynaPro® NanoStar™ (Wyatt Technology) using settings suggested by the manufacturer. A fit of the second order autocorrelation function to a globular protein model was used to derive the hydrodynamic radius and plotted on Graphpad Prism 9.3.1.

Mosaic-8b RBD-mi3 and homotypic SARS-2 RBD-mi3 were compared by negative-stain EM. Ultrathin, holey carbon-coated, 400 mesh Cu grids (Ted Pella, Inc.) were glow discharged (60 s at 15 mA), and a 3 μ L aliquot of SEC-purified RBD-mi3 nanoparticles were diluted to ~40-100 μ g/mL and applied to the grids for 60 s. Grids were then negatively stained with 2% (w/v) uranyl acetate for 30 s. Images were collected with a 120 keV FEI Tecnai T12 transmission electron microscope at 42,000x magnification.

K18-hACE2 mice. The Institutional Animal Care and Use Committee at Rocky Mountain Laboratories provided animal study approvals, which were conducted in an Association for Assessment and Accreditation of Laboratory Animal Care-accredited facility, following the basic principles and guidelines in the *Guide for the Care and Use of Laboratory Animals* eighth edition, the Animal Welfare Act, U.S. Department of Agriculture, and the U.S. Public Health Service Policy on Humane Care and Use of Laboratory Animals.

Animals were kept in climate-controlled rooms with a fixed light/dark cycle (12 hours/12 hours). Mice were cohoused in rodent cages, fed a commercial rodent chow with *ad libitum* water, and monitored at least once daily. The Institutional Biosafety Committee (IBC)–approved work with infectious SARS-1 and SARS-2 viruses was conducted under biosafety level 3 (BSL3) conditions. All sample inactivation was performed according to IBC-approved standard operating procedures for removal of specimens from high containment.

Cells and virus for K18-hACE2 mouse studies. Virus propagation was performed in VeroE6 cells in DMEM containing 2% FBS, 1 mM L-glutamine, penicillin (50 U/mL), and streptomycin (50 µg/mL (DMEM2). The consensus sequence of the virus stock (SARS-CoV-2 Beta, isolate hCoV-19/USA/MD-HP01542/2021) used for these experiments was identical to the initial sequence deposited on GISAID (EPI_ISL_890360), and no contaminants or additional mutations were detected. VeroE6 cells were maintained in DMEM supplemented with 10% fetal bovine serum, 1 mM L-glutamine, penicillin (50 U/mL), and streptomycin (50 µg/mL). VeroE6 cells were provided by R. Baric (University of North Carolina at Chapel Hill). Mycoplasma testing is performed at monthly intervals, and no mycoplasma was detected.

Vaccination and infection of K18-hACE2 mice. K18-hACE2 mice (4 to 6 weeks old) were vaccinated with 2 x 50 µL of 5 µg (RBD equivalents)/(11.4 µg of total RBD-mi3) of RBD-mi3 or 5 µg unconjugated mi3 adjuvanted with Addavax 1:1 (1:1 v/v) intramuscularly at day 0 and day 28 (and challenged 28 days post the second immunization). Fourteen days before virus challenge, animals were bled via the submandibular vein. 10 animals per group were challenged with 30 µL of 10⁵ TCID₅₀ SARS-2/human/USA/MD-HP01542/2021) or SARS-1 (Tor2) diluted in sterile Dulbecco's modified Eagle's medium (DMEM). Weight was recorded daily. Six mice per group were observed for survival up to 28 days post challenge or until they reached end-point criteria. End-point criteria were as follows: labored breathing or ambulatory difficulties or weight loss exceeding 20%. Four animals per group were euthanized on day 4 post challenge to collect oropharyngeal swabs and lung tissue for virology and histology analysis.

Virus titration after K18-hACE2 mouse challenge. Lung tissue sections were weighed and homogenized in 750 µL of DMEM. Virus titrations were performed by end point titration in VeroE6 cells expressing transmembrane protease serine 2 (TMPRSS-2) and human ACE2 (BEI resources, NR-54970), which were inoculated with 10-fold serial dilutions of virus swab medium or tissue homogenates in 96-well plates. When titrating tissue homogenate, cells were washed with PBS and 100 µL of DMEM2. Cells were incubated at 37°C and 5% CO₂, and cytopathic effect (CPE) was assessed 6 days later.

RNA extraction and quantitative RT-PCR. RNA was extracted from oropharyngeal swabs using a QIAamp Viral RNA kit (Qiagen) according to the manufacturer's instructions. Tissue was homogenized and extracted using the RNeasy kit (Qiagen) according to the manufacturer's instructions. Viral gRNA- and sgRNA-specific assays (47) were used for the detection of viral RNA. The RT-PCR reaction (with 5 µL template viral RNA) was performed using the QuantStudio (Thermo Fisher Scientific) according to instructions of the manufacturer. Dilutions of SARS-2 with known genome copies were run in parallel to be used to generate the standard curves.

Histopathology of K18-hACE2 mouse samples. Lungs were collected upon necropsy on day 4 post challenge and perfused with 10% neutral-buffered formalin. Fixation was done for at least 7 days. Tissues were placed in cassettes and processed with a Sakura VIP-6 Tissue Tek on a 12-hour automated schedule using a graded series of ethanol, xylene, and PureAffin. Embedded tissues were sectioned at 5µm and dried overnight at 42 degrees C prior to staining. Sections

were stained with Harris hematoxylin (Cancer Diagnostics, no. SH3777), decolorized with 0.125% HCl/70% ethanol, blued in Pureview PH Blue (Cancer Diagnostics, no. 167020), counterstained with eosin 615 (Cancer Diagnostics, no. 16601), dehydrated, and mounted in Micromount (Leica, no. 3801731). An anti-SARS-2 nucleocapsid protein rabbit antiserum (generated by GenScript) was used at a 1:1000 dilution to detect specific anti-SARS-2 immunoreactivity using the Discovery ULTRA automated staining instrument (Roche Tissue Diagnostics) with a Discovery ChromoMap DAB (Ventana Medical Systems) kit. All slides were examined by a board-certified veterinary anatomic pathologist who was blinded to study group allocations. Scoring was done as follows. H&E; no lesions = 0; less than 1% = 0.5; minimal (1-10%) = 1; mild (11-25%) = 2; moderate (26-50%) = 3; marked (51-75%) = 4; severe (76-100%) = 5. IHC attachment; none = 0; less than 1% = 0.5; rare/few (1-10%) = 1; scattered (11-25%) = 2; moderate (26-50%) = 3; numerous (51-75%) = 4; diffuse (76-100%) = 5. Histopathology report is summarized in Data S1.

BIOQUAL Ethics Statement and Animal Exposure. Rhesus macaques were housed and cared for at BIOQUAL, Inc., Rockville, MD. The study was performed under a BIOQUAL-approved IACUC protocol (no. 21-092P), in strict accordance with the recommendations in the Guide for the Care and Use of Laboratory Animals of the NIH, and in accordance with BIOQUAL standard operating procedures. BIOQUAL is fully accredited by the Association for Assessment and Accreditation of Laboratory Animal Care (AAALAC) and through OLAW, assurance number A-3086. All animal procedures were done under anesthesia to minimize pain and distress, in accordance with the recommendations of the Weatherall report 'The use of non-human primates in research.' Teklad 5038 primate diet was provided once daily according to macaque size and weight. The diet was supplemented daily with fresh fruit and vegetables. Fresh water was given *ad libitum*.

Vaccination of NHPs. The study included 16 rhesus macaques (*Macaca mulatta*), 8 of which were immunized with mosaic-8b RBD-mi3 (n = 8), and 8 of which served as unimmunized controls for SARS-2 and SARS-1 challenges. Four immunized and four unimmunized control NHPs were challenged with SARS-2, and four immunized and four unimmunized control NHPs were challenged with SARS-1. Due to a shortage of available NHPs, we could not compare mosaic-8b RBD-mi3 and homotypic SARS-2 Beta RBD-mi3 immunizations in this study. Macaques were 3-5 years old and ranged from 3.2 to 5.1 kg in body weight. Male and female macaques per group were balanced. Studies were performed unblinded. Macaques were evaluated by BIOQUAL veterinary staff before, during, and after immunizations.

NHPs were immunized intramuscularly with 25 µg (calculated based on RBDs; 56.8 µg of total RBD-mi3) of mosaic-8b RBD-mi3 adjuvanted with VAC20 (2% aluminum hydroxide wet gel, Al₂O₃) (alum) (Prime and Boost 1) (kind gift of Francis Laurent and Ruben Caputo, SPI Pharma) and subsequently with MF59 adjuvant (EmulsiPan, a squalene-based oil in water emulsion adjuvant (50) (kind gift of Harshet Jain, Panacea Biotec) for Boost 2. Each macaque received 0.5 mL into the right forelimb.

SARS-2 and SARS-1 intranasal and intratracheal NHP challenges. All macaques were challenged at week 11 (3 weeks after last vaccination) through combined intratracheal (1.0 mL) and intranasal (0.5 mL per nostril) inoculation with an infectious dose of 10⁵ TCID₅₀ of SARS-2 B.1.617.2 (Delta, BEI NR-55612) or SARS-1 (Urbani). Virus was stored at -80 °C before use, thawed by hand and placed immediately on wet ice. Stock was diluted to 5 × 10⁴ TCID₅₀ mL⁻¹ in PBS and vortexed gently for 5 s before inoculation. Nasal swabs, BAL, plasma, and serum samples were collected seven days before and two and four days after challenge. Protection from SARS-2 and SARS-1 infection was determined by quantitative infectious viral load assay

(TCID₅₀), and for SARS-2, also by RT-PCR of subgenomic N RNA (N sgRNA) as described above except that amplification was done use the Applied Biosystems 7500 Sequence detector.

TCID₅₀ and SARS-2 and SARS-1 virus PRNT₅₀ assays in NHP samples

PRNT₅₀ (50% plaque reduction neutralization test) assays for NHP samples were performed in a biosafety level 3 facility at BIOQUAL, Inc. (Rockville, MD). The TCID₅₀ assay was conducted by addition of 10-fold graded dilutions of samples to Vero/TMPRSS2 cell monolayers. Serial dilutions were performed in cell culture wells in quadruplicates. Positive (virus stock of known infectious titer in the assay) and negative (medium only) control wells were included in each assay set-up. The plates were incubated at 37°C, 5.0% CO₂ for 4 days. The cell monolayers were visually inspected for CPE, i.e., complete destruction of the monolayer. TCID₅₀ values was calculated using the Reed-Muench formula (85). For samples that had less than 3 CPE positive wells, the TCID₅₀ could not be calculated using the Reed-Muench formula, and these samples were assigned a titer of below the limit of detection (i.e., <2.7 log₁₀ TCID₅₀/mL). For acceptable assay performance, the TCID₅₀ value of the positive control tested within 2-fold of the expected value.

To measure neutralization activity, sera from each NHP were diluted to 1:10 followed by a 3-fold serial dilution. Diluted samples were then incubated with ~30 plaque-forming units of wild-type SARS-2 USA-WA1/2020 (BEI NR-52281), B.1.351 (Beta, 501Y.V2.HV, NR-54974), or B.1.617.2 (Delta, BEI NR-55612) variants, in an equal volume of culture medium for 1 hour at 37°C. The serum-virus mixtures were added to a monolayer of confluent Vero E6 cells and incubated for one hour at 37°C in 5% CO₂. Each well was then overlaid with culture medium containing 0.5% methylcellulose and incubated for 3 days at 37°C in 5% CO₂. The plates were then fixed with methanol at -20°C for 30 minutes and stained with 0.2% crystal violet for 30 min at room temperature. PRNT₅₀ were estimated by determining the dilution at which plaques were reduced by 50% with respect to viral control.

Mouse and NHP serum ELISAs. 20 µL of a 2.5 µg/mL solution of an affinity purified His-tagged RBD in 0.1 M NaHCO₃ pH 9.8 was coated onto Nunc® MaxiSorp™ 384-well plates (Sigma) and incubated overnight at 4°C. After blocking with 3% bovine serum albumin (BSA) in TBS containing 0.1% Tween 20 (TBS-T) for 1 hr at room temperature, plates were washed with TBS-T, and mouse or NHP serum diluted 1:100 and then serially diluted by 4-fold with TBS-T/3% BSA was added to the plates for 3 hr at room temperature. Plates were then washed again for 1 hr at room temperature, and a 1:50,000 dilution of secondary HRP-conjugated goat anti-mouse IgG (Abcam) was added. SuperSignal™ ELISA Femto Maximum Sensitivity Substrate (ThermoFisher) was added to plates following manufacturer's instructions, and plates were read at 425 nm. Curves were plotted and analyzed to obtain midpoint titers (EC₅₀ values) using Graphpad Prism 9.3.1 (Graphpad Software, San Diego, CA) assuming a one-site binding model with a Hill coefficient. Titer differences were evaluated for statistical significance between groups using ANOVA test followed by Tukey's multiple comparison post hoc test calculated using Graphpad Prism 9.3.1.

Mouse and NHP serum pseudovirus neutralization assays. Lentiviral-based SARS-2 variants (Wuhan-Hu-1, Beta, Delta, Omicron BA.1), SARS-1, WIV1, SHC014, and BtKY72 K493Y/T498W (13) (kind gift of Alexandra Walls and David Velesler, University of Washington) pseudoviruses were prepared as described (20, 86) using genes encoding S protein sequences lacking C-terminal residues in the cytoplasmic tail: 21 amino acid deletions for SARS-2 variants, WIV1, SHC014, and BtKY72 and a 19 amino acid deletion for SARS-CoV. For neutralization assays, three-fold serially diluted sera from immunized mice or NHPs were incubated with a pseudovirus for 1 hour at 37°C, then the serum/virus mixture was added to 293T_{ACE2} target cells and incubated for 48 hours at 37°C. Media was removed, cells were lysed with Britelite Plus reagent (Perkin Elmer), and luciferase activity was measured as relative luminescence units (RLUs). Relative RLUs

were normalized to RLUs from cells infected with pseudotyped virus in the absence of antiserum. Half-maximal inhibitory dilutions (ID_{50} values) were derived using 4-parameter nonlinear regression in AntibodyDatabase (87). Statistical significance of titer differences between groups were evaluated using ANOVA test followed by Tukey's multiple comparison post hoc test of ID_{50} s converted to log₁₀ scale using Graphpad Prism 9.3.1.

Mouse serum samples for RBD epitope mapping. Animal procedures and experiments were performed at Labcorp Drug Development (formerly Covance, Inc.) according to protocols approved by the IACUC to obtain serum samples for RBD epitope mapping experiments. Immunizations of mosaic-8b or homotypic SARS-2 Beta (5 µg each based on RBD content, 11.4 µg of total RBD-mi3) in 100 µL of 50% v/v AddaVax™ adjuvant (InvivoGen) were done using intramuscular (IM) injections of 7-8-week-old female BALB/c mice (Envigo) (8 animals per cohort). Animals were boosted 3 weeks after the prime with the same quantity of antigen in adjuvant. Animals were bled under anesthesia approximately every 2 weeks via orbital sinus and then euthanized 7 weeks after the prime (Day 49) after blood collection from the jugular vein. Blood samples were stored at room temperature in serum separator tubes (BD Microtainer) to allow clotting. Serum was then harvested into microtubes (Mikro-Schraubrohre) and stored at -80°C until use.

RBD sequencing library construction and SARS-2 enrichment. To construct sequencing libraries for RBD epitope mapping of mouse sera, 25 µL of ds-cDNA was brought to a final volume of 53 µL in elution buffer (Agilent Technologies) and sheared on a Covaris LE220 (Covaris) to generate an average size of 180 to 220 base pairs (bp). The following settings were used: peak incident power, 450 W; duty factor, 15%; cycles per burst, 1000; and time, 300 s. The Kapa HyperPrep kit was used to prepare libraries from 50 µL of each sheared cDNA sample following modifications of the Kapa HyperPrep kit (version 8.20) and SeqCap EZ HyperCap Workflow (version 2.3) user guides (Roche Sequencing Solutions Inc.). Adapter ligation was performed for 1 hour at 20°C using the Kapa Unique-Dual Indexed Adapters diluted to 1.5 µM concentration (Roche Sequencing Solutions Inc.). After ligation, samples were purified with AmPure XP beads (Beckman Coulter) and subjected to double-sided size selection as specified in the SeqCap EZ HyperCap Workflow User's Guide. Precapture polymerase chain reaction (PCR) amplification was performed using 12 cycles, followed by purification using AmPure XP beads. Purified libraries were assessed for quality on the Bioanalyzer 2100 using the High-Sensitivity DNA chip assay (Agilent Technologies). Quantification of pre-capture libraries was performed using the Qubit dsDNA HS Assay kit and the Qubit 3.0 fluorometer following the manufacturer's instructions (Thermo Fisher Scientific).

The myBaits Expert Virus bait library was used to enrich samples for SARS-2 according to the myBaits Hybridization Capture for Targeted NGS (version 4.01) protocol. Briefly, libraries were sorted according to estimated genome copies and pooled to create a combined mass of 2 µg for each capture reaction. Depending on estimated genome copies, two to six libraries were pooled for each capture reaction. Capture hybridizations were performed for 16 to 19 hours at 65°C and subjected to 8 to 14 PCR cycles after enrichment. SARS-2-enriched libraries were purified and quantified using the Kapa Library Quant Universal quantitative PCR mix in accordance with the manufacturer's instructions. Libraries were diluted to a final working concentration of 1 to 2 nM, titrated to 20 pM, and sequenced as 2 × 150 bp reads on the MiSeq sequencing instrument using the MiSeq Micro kit version 2 (Illumina).

Sorting of yeast libraries to identify mutations that reduced binding by polyclonal antisera. Plasma mapping experiments were performed in biological duplicate using the independent mutant RBD libraries as previously described (44). Prior to the yeast-display deep mutational

scanning experiments, 100 μ L of each serum sample was heat-inactivated at 56°C for 30 min and twice-depleted of nonspecific yeast-binding antibodies by incubating with 50 OD units of AWY101 yeast containing an empty vector (54). Mutant yeast libraries that were pre-sorted for RBD expression and ACE2 binding (54) were induced to express RBD in galactose-containing synthetic defined medium with casamino acids (6.7g/L Yeast Nitrogen Base, 5.0g/L Casamino acids, 1.065 g/L MES acid, and 2% w/v galactose + 0.1% w/v dextrose). 16–18 hours post-induction, cells were washed and incubated with plasma at a range of dilutions for 1 hour at room temperature with gentle agitation. For each plasma, we chose a sub-saturating dilution such that the amount of fluorescent signal due to plasma antibody binding to RBD was approximately equal across samples. The exact dilution used for each plasma is given in fig. S5B. The libraries were washed and secondarily labeled for 1 hour with 1:100 fluorescein isothiocyanate-conjugated anti-MYC antibody (Immunology Consultants Lab, CYMC-45F) to label for RBD expression and 1:200 Alexa Fluor-647-conjugated goat anti-human-IgG Fc-gamma (Jackson ImmunoResearch 109-135-098) to label for bound NHP antibodies or Alexa Fluor-647-conjugated goat anti-mouse-IgG Fc-gamma (Jackson ImmunoResearch 115-605-008) to label for bound mouse antibodies. A flow cytometric selection gate was drawn to capture RBD mutants with reduced antibody binding for their degree of RBD expression (fig. S5C). For each sample, 7.5×10^6 to 1.1×10^7 cells were processed on the BD FACSAria II cell sorter (fig. S5C). Antibody-escaped cells were grown overnight in synthetic defined medium with casamino acids (6.7g/L Yeast Nitrogen Base, 5.0g/L Casamino acids, 1.065 g/L MES acid, and 2% w/v dextrose + 100 U/mL penicillin + 100 μ g/mL streptomycin) to expand cells prior to plasmid extraction.

DNA extraction and Illumina sequencing. Plasmid samples were prepared from 30 optical density (OD) units (1.6×10^8 colony forming units (cfus)) of pre-selection yeast populations and approximately 5 OD units ($\sim 3.2 \times 10^7$ cfus) of overnight cultures of plasma-escaped cells (Zymoprep Yeast Plasmid Miniprep II) as previously described (53, 88). The 16-nucleotide barcode sequences identifying each RBD variant were amplified by polymerase chain reaction (PCR) and prepared for Illumina sequencing as described (53, 88). Barcodes were sequenced on an Illumina HiSeq 2500 with 50 bp single-end reads. Raw sequencing data are available on the NCBI SRA under BioProject PRJNA770094, BioSample SAMN26315988.

Analysis of deep sequencing data to compute each mutation's escape fraction. Escape fractions were computed essentially as described in (53) and exactly as described in (54). We used the `dms_variants` package (https://jbloomlab.github.io/dms_variants/, version 0.8.10) to process Illumina sequences into counts of each barcoded RBD variant in each pre-selection and antibody-escape population. We computed the escape fraction for each barcoded variant using the deep sequencing counts for each variant in the original and plasma-escape populations and the total fraction of the library that escaped antibody binding via the formula in (54). These escape fractions represent the estimated fraction of cells expressing that specific variant that falls in the escape bin, such that a value of 0 means the variant is always bound by plasma and a value of 1 means that it always escapes plasma binding.

We then applied a computational filter to remove variants with >1 amino-acid mutation, low sequencing counts, or highly deleterious mutations that might escape antibody binding due to poor RBD expression or folding as described (54). The reported antibody-escape scores are the average across duplicate libraries; these scores are also in Data S2. Correlations in final single-mutant escape scores are shown in fig. S5D. Full documentation of the computational analysis is at https://github.com/jbloomlab/SARS-CoV-2-RBD_Beta_mosaic_np_vaccine.

Data visualization. The static logo plot visualizations of the escape maps in the paper figures were created using the `dmslogo` package (<https://jbloomlab.github.io/dmslogo>, version 0.6.2) and

in all cases the height of each letter indicates the escape fraction for that amino-acid mutation calculated as described above. For the mouse sera, the static logo plots feature any site where for ≥ 1 serum, the site-total antibody escape was $>10x$ the median across all sites and at least 10% the maximum of any site. Due to the relative breadth of the NHP sera, a more sensitive threshold for displaying sites on logo plots was used: we include any site where the site-total antibody escape is $>5x$ the median across all sites and at least 5% maximum of any sites. This resulted in sites 383, 386, and 500. Thus, sites 346, 352, 357, 369, 378, 384, 385, 390, 396, 408, 462, 468, 477, 478, 484, 485, 486, and 501 were also added to the logo plots to facilitate comparison to the mouse sera. For each sample, the y-axis is scaled to be the greatest of (a) the maximum site-wise escape metric observed for that sample, or (b) $20x$ the median site-wise escape fraction observed across all sites for that plasma. The code that generates these logo plot visualizations is available at https://github.com/jbloomlab/SARS-CoV-2-RBD_Beta_mosaic_np_vaccine/blob/main/results/summary/escape_profiles.md. In many of the visualizations, the RBD sites are categorized by epitope region (23) and colored accordingly. Specifically, we define the class 1 epitope as residues 403+405+406+417+420+421+453+455–460+473–478+486+487+489+503+504, the class 2 epitope as residues 472+479+483–485+490–495, the class 3 epitope to be residues 341+345+346+354–357+396+437-452466–468+496+498–501, and the class 4 epitope as residues 365–390+408+462.

For the static structural visualizations in figures, the Beta RBD surface (PDB 7LYQ) was colored by the site-wise escape metric at each site, with white indicating no escape and red scaled to be the same maximum used to scale the y-axis in the logo plot escape maps, determined as described above. We created interactive structure-based visualizations of the escape maps using dms-view (89) that are available at https://jbloomlab.github.io/SARS-CoV-2-RBD_Beta_mosaic_np_vaccine/.

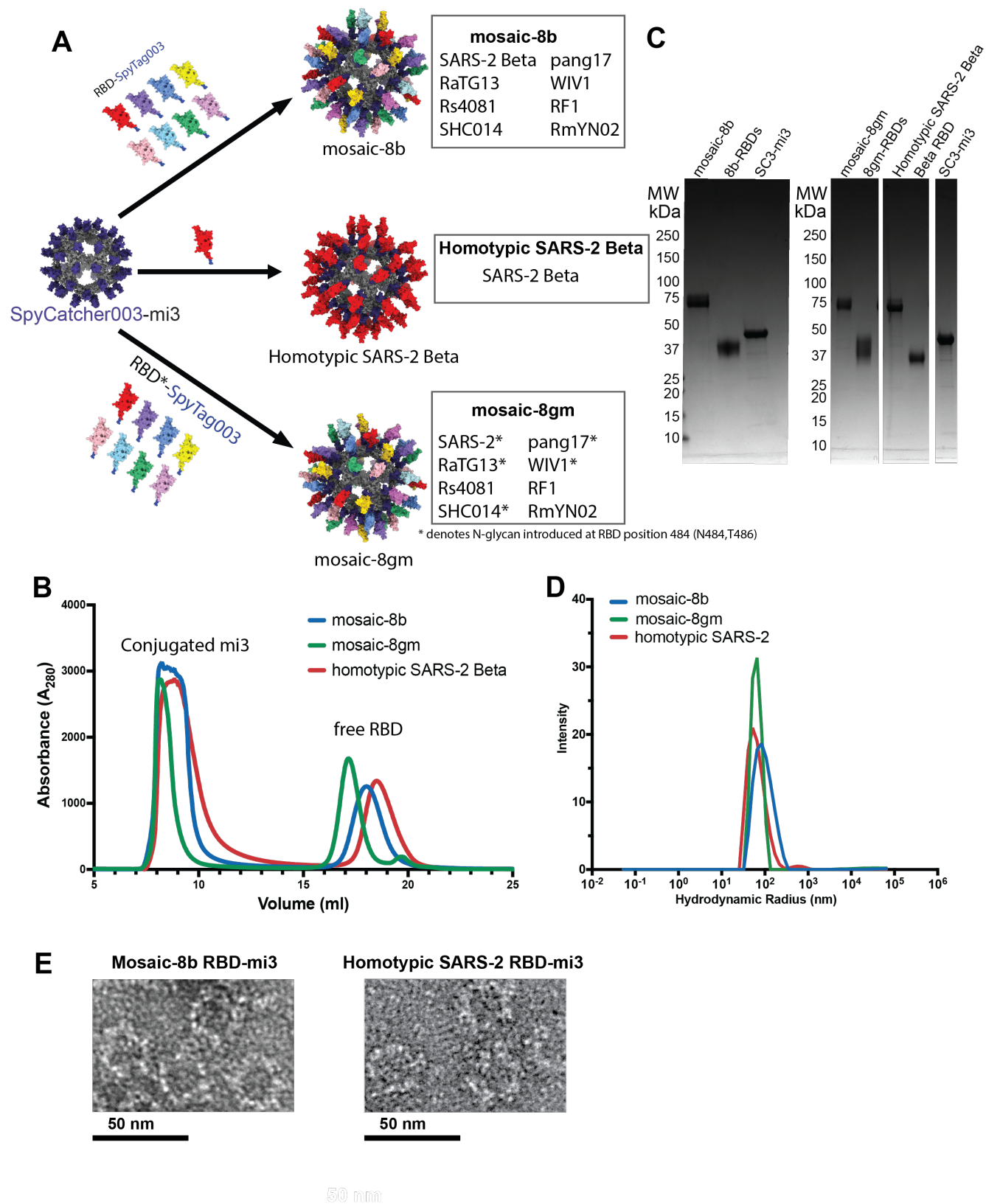
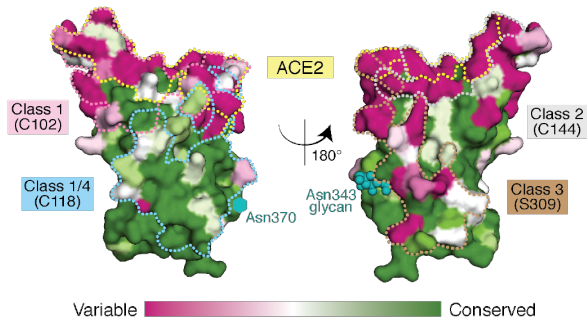
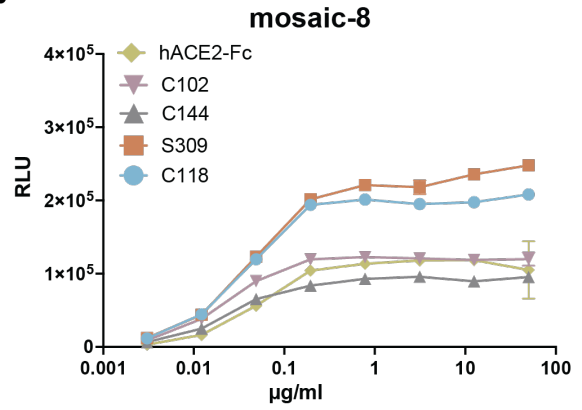


Figure S1. Preparation of RBD-mi3 nanoparticles. **(A)** Schematic for construction of mosaic-8b, mosaic-8gm, and homotypic SARS-2 Beta RBD-mi3 nanoparticles. **(B)** Superose 6 10/300 SEC profile after RBD conjugations to mi3 (2-fold molar excess of RBD to mi3 subunit) showing peaks for RBD-mi3 nanoparticles and free RBD(s). **(C)** SDS-PAGE (Coomassie staining) of RBD-coupled nanoparticles, free RBDs, and free SpyCatcher003-mi3 particles (SC3-mi3). **(D)** Dynamic light scattering (DLS) measurements for RBD-coupled nanoparticles. **(E)** Negative-stain EM images of RBD-coupled mi3 nanoparticles.

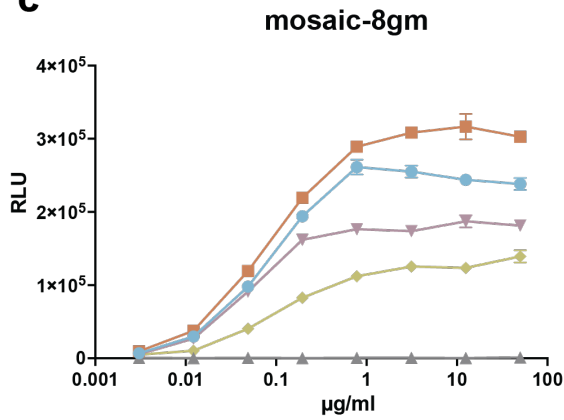
A



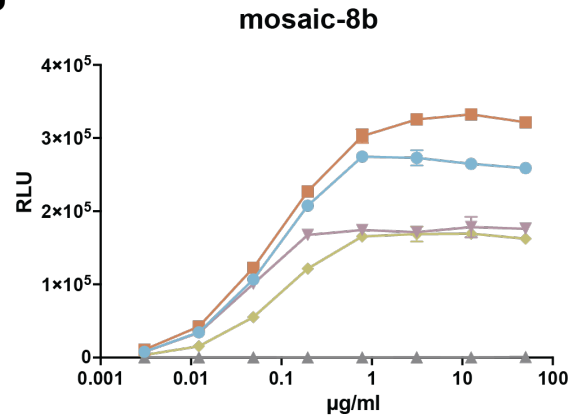
B



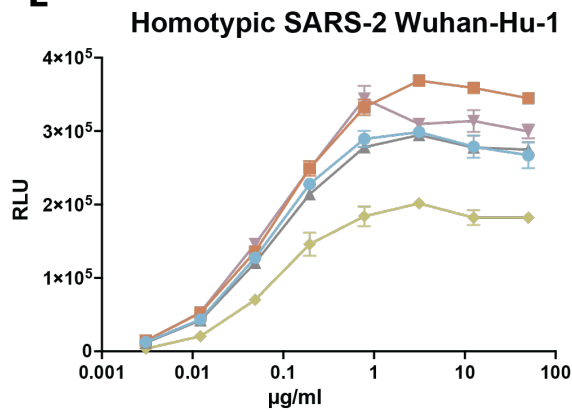
C



D



E



F

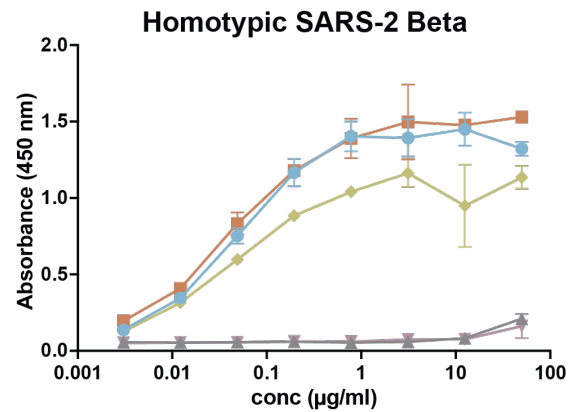


Figure S2. Binding characteristics of mosaic and homotypic RBD-mi3 nanoparticles. **(A)** Sequence conservation of the 16 sarbecovirus RBDs in Fig. 1D calculated by the ConSurf Database (79) shown on two views of an RBD surface (PDB 7BZ5). The ACE2 binding footprint (PDB 6M0J) is outlined by yellow dots. Epitopes of representative monoclonal antibodies used in binding experiments are outlined in dots of the indicated colors using information from structures of Fabs bound to RBD or S trimer (C118: PDB 7RKS, S309: PDB 7JX3; C144: PDB 7K90, C102: PDB 7K8M). The N-linked glycan attached to RBD residue 343 is indicated by teal spheres, and the potential N-linked glycosylation site at position 370 in RBDs derived from sarbecoviruses other than SARS-2 is indicated by a teal circle. **(B-F)** ELISAs to assess binding of the hACE2-Fc and the indicated monoclonal antibodies to RBD-mi3 nanoparticles. Nanoparticles were immobilized on an ELISA plate, incubated with the indicated monoclonal antibody or hACE2-Fc, and binding was detected using a labeled anti-human IgG secondary antibody. Data points are presented as the mean and standard deviation of duplicate measurements. Some error bars are too small to be distinguished from data points. RLU = relative luminescence units. **(B)** Binding to mosaic-8 RBD-mi3 (Wuhan-Hu-1 SARS-2 RBD plus seven animal sarbecovirus RBDs as previously described (34) and in fig. S1A). **(C)** Binding to mosaic-8gm RBD-mi3 (mosaic-8 with a Wuhan-Hu-1 SARS-2 RBD plus the seven animal sarbecovirus RBDs in which N-linked glycosylation site sequons at RBD position 484 were introduced in the clade 1a and 1b RBDs to occlude class 1 and 2 RBD epitopes). **(D)** Binding to mosaic-8b RBD-mi3 (SARS-2 Beta RBD plus the seven animal sarbecovirus RBDs in fig. S1A). **(E)** Binding to homotypic SARS-2 Wuhan Hu-1 RBD-mi3 (as previously described (34)). **(F)** Binding to homotypic SARS-2 Beta RBD-mi3.

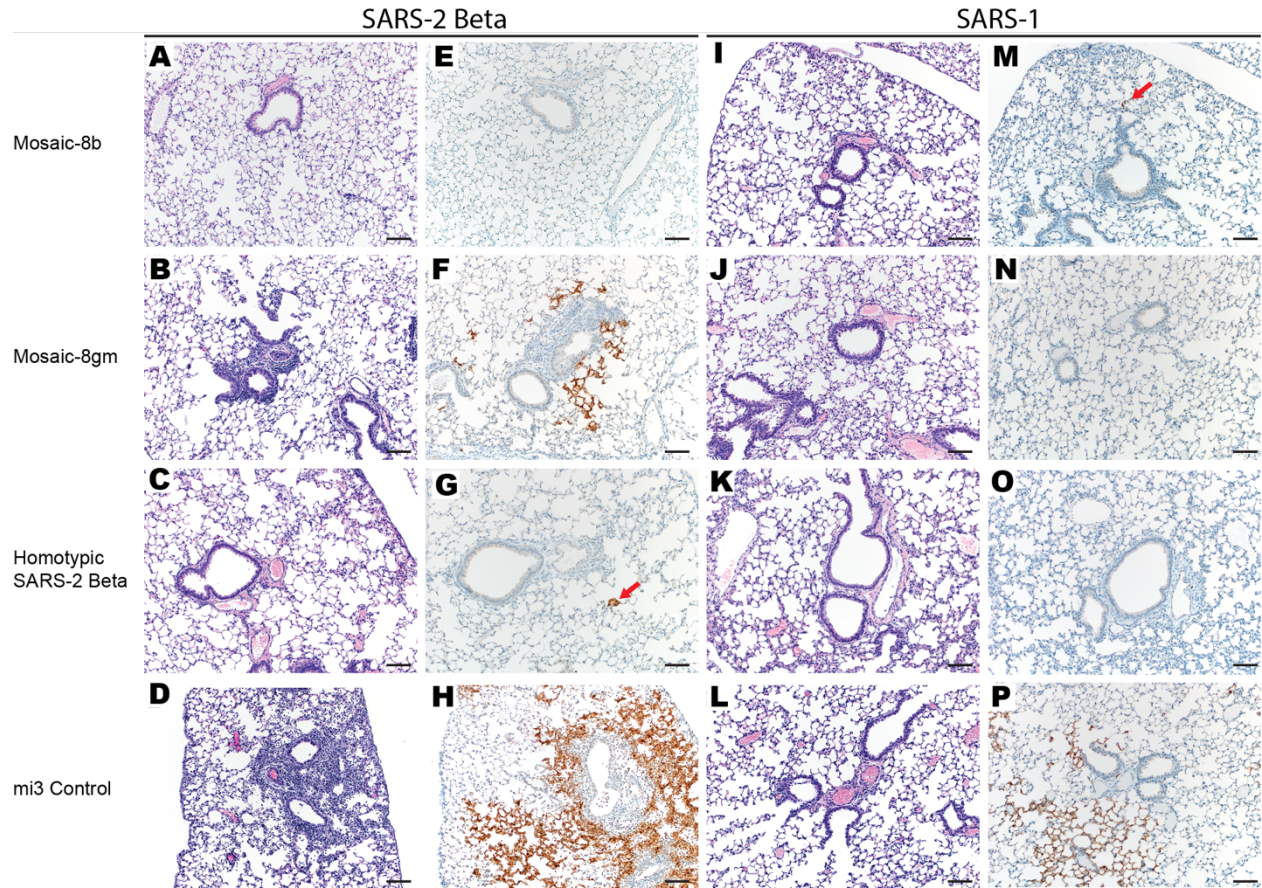


Figure S3. Lung pathology is reduced in mosaic-8b immunized mice challenged with either SARS-2 or SARS-1. Images taken at 100x magnification. Scale bar = 100 μ m. Red arrows = immunoreactivity in panels G and M. **(A-D)** Hematoxylin and eosin (H&E) stained lung tissue sections from animals vaccinated with either mosaic-8b, mosaic-8gm, homotypic SARS-2 Beta, or unconjugated mi3 and challenged with SARS-2 Beta (minimal-mild peribronchial inflammation in panels B and D). **(E-H)** Immunohistochemistry (IHC) staining for SARS-CoV-2 N protein antigen from animals vaccinated with either mosaic-8b, mosaic-8gm, homotypic SARS-2 Beta, or mi3 and challenged with SARS-2 Beta. **(I-L)** H&E stained lung tissue sections from animals vaccinated with either mosaic-8b, mosaic-8gm, homotypic SARS-2 Beta, or mi3 and challenged with SARS-1. **(M-P)** Immunohistochemistry staining for SARS-CoV-2 N protein antigen from animals vaccinated with either mosaic-8b, mosaic-8gm, homotypic SARS-2 Beta, or mi3 and challenged with SARS-1.

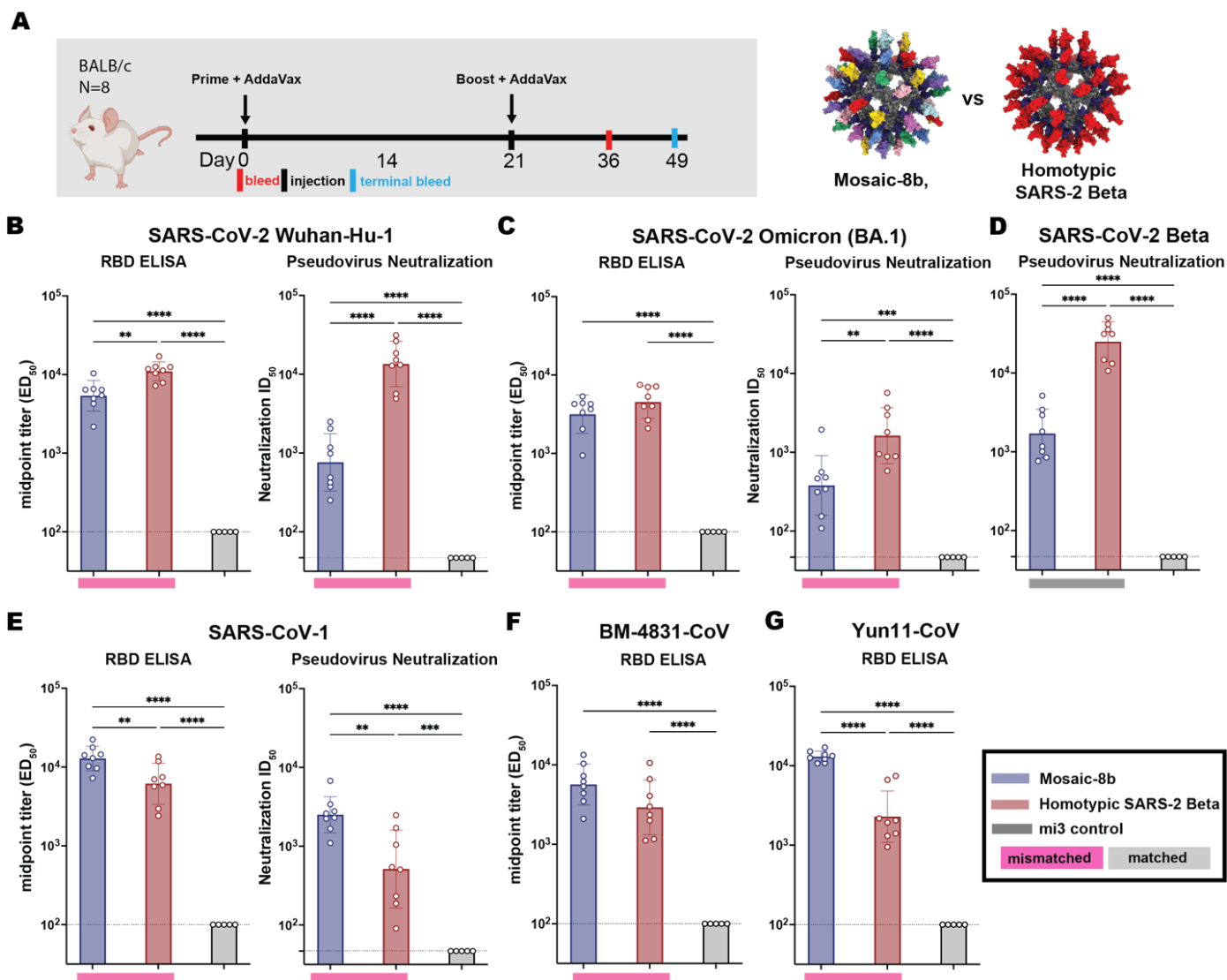


Figure S4. Mosaic-8b and homotypic SARS-2 Beta RBD-mi3 immunizations elicit binding and neutralizing antibodies in BALB/c mice. **(A)** Left: Immunization schedule. BALB/c mice were immunized with either mosaic-8 or homotypic SARS-2 Beta RBD-mi3. Right: Structural models of mosaic-8 and homotypic RBD-mi3 nanoparticles constructed using PDB 7SC1 (RBD), PDB 4MLI (SpyCatcher), and PDB 7B3Y (mi3). **(B-G)** ELISA and neutralization data for antisera (taken 4 weeks post boost) from individual mice (open circles) presented as the mean (bars) and standard deviation (horizontal lines). ELISA results are shown as midpoint titers (EC_{50} values); neutralization results are shown as half-maximal inhibitory dilutions (ID_{50} values). Dashed horizontal lines correspond to the background values representing the limit of detection. Significant differences between cohorts linked by horizontal lines are indicated by asterisks: $p < 0.05 = *$, $p < 0.01 = **$, $p < 0.001 = ***$, $p < 0.0001 = ****$. Rectangles below ELISA and neutralization data indicate mismatched strains (pink; the RBD from that strain was not present on the nanoparticle) or matched strains (gray; the RBD was present on the nanoparticle).

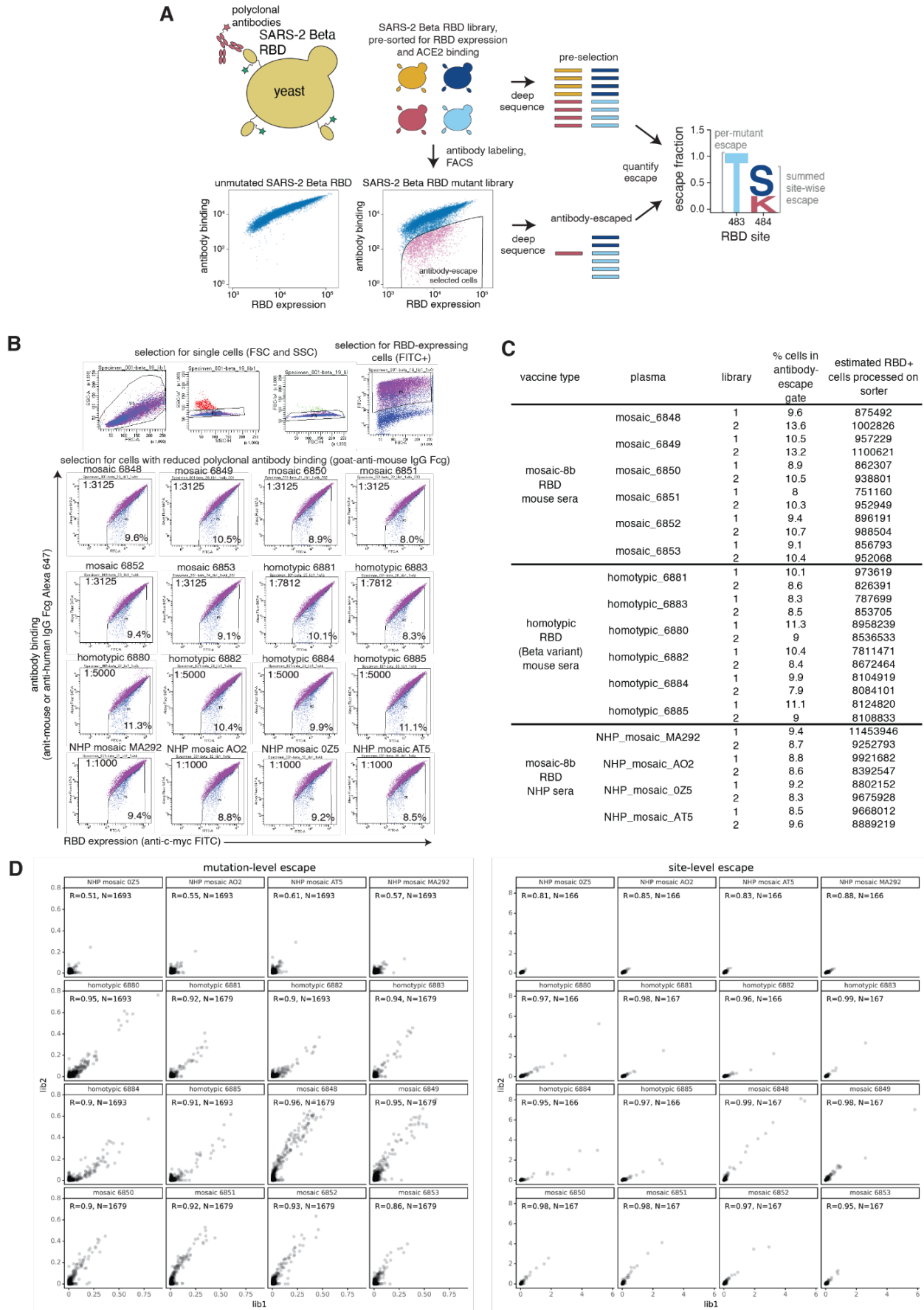


Figure S5. Comprehensive mapping of mutations that reduce binding of sera from immunized mice or NHPs to the SARS-2 Beta RBD. **(A)** Deep mutational scanning (54) was used to map mutations that reduced binding of polyclonal antibodies from immunized animals to the SARS-2 Beta RBD. A library of yeast containing nearly all possible mutations in the SARS-2 Beta RBD was incubated with sera from immunized mice or NHPs, and fluorescence-activated cell sorting (FACS) was used to enrich for cells expressing RBD (detected with a C-terminal Myc tag, green star) with reduced antibody binding, detected using an anti-mouse (for mouse sera) or anti-human (for NHP sera) IgG Fc-gamma secondary antibody. Deep sequencing was used to quantify the frequency of each mutation in the pre-selection and antibody-escape cell populations. We calculated each mutation's "escape fraction," the fraction of cells expressing RBD with that mutation that fell in the antibody-escape FACS bin (ranging from 0 to 1). The site-level escape metric is the sum of the escape fractions of all mutations at a site. **(B)** Top: Representative plots of nested FACS gating strategy used for all experiments to select for RBD+ single cells. Samples were gated by SSC-A versus FSC-A, SSC-W versus SSC-H, and FSC-W versus FSC-H) that also express RBD (FITC-A vs. FSC-A). Bottom: FACS gating strategy for one of two independent libraries to select cells expressing RBD mutants with reduced binding by polyclonal sera (cells in blue). Gates were set manually during sorting. Selection gates were set to capture cells that have a reduced amount of antibody binding for their degree of RBD expression. FACS scatter plots were qualitatively similar between the two libraries. SSC-A, side scatter-area; FSC-A, forward scatter-area; SSC-W, side scatter-width; SSC-H, side scatter-height; FSC-W, forward scatter-width; FSC-H, forward scatter height; FITC-A, fluorescein isothiocyanate-area. **(C)** The percent and number of RBD+ cells sorted into the antibody-escape gate for each library selected against each serum. **(D)** Mutation (top)- and site (bottom)-level correlations of escape scores between two independent biological replicate libraries. The complete antibody-escape scores are available in [Data S2](#) and at [https://github.com/jbloomlab/SARS-CoV-2-RBD Beta mosaic np vaccine/blob/main/results/supp_data/all_raw_data.csv](https://github.com/jbloomlab/SARS-CoV-2-RBD_Beta_mosaic_np_vaccine/blob/main/results/supp_data/all_raw_data.csv).

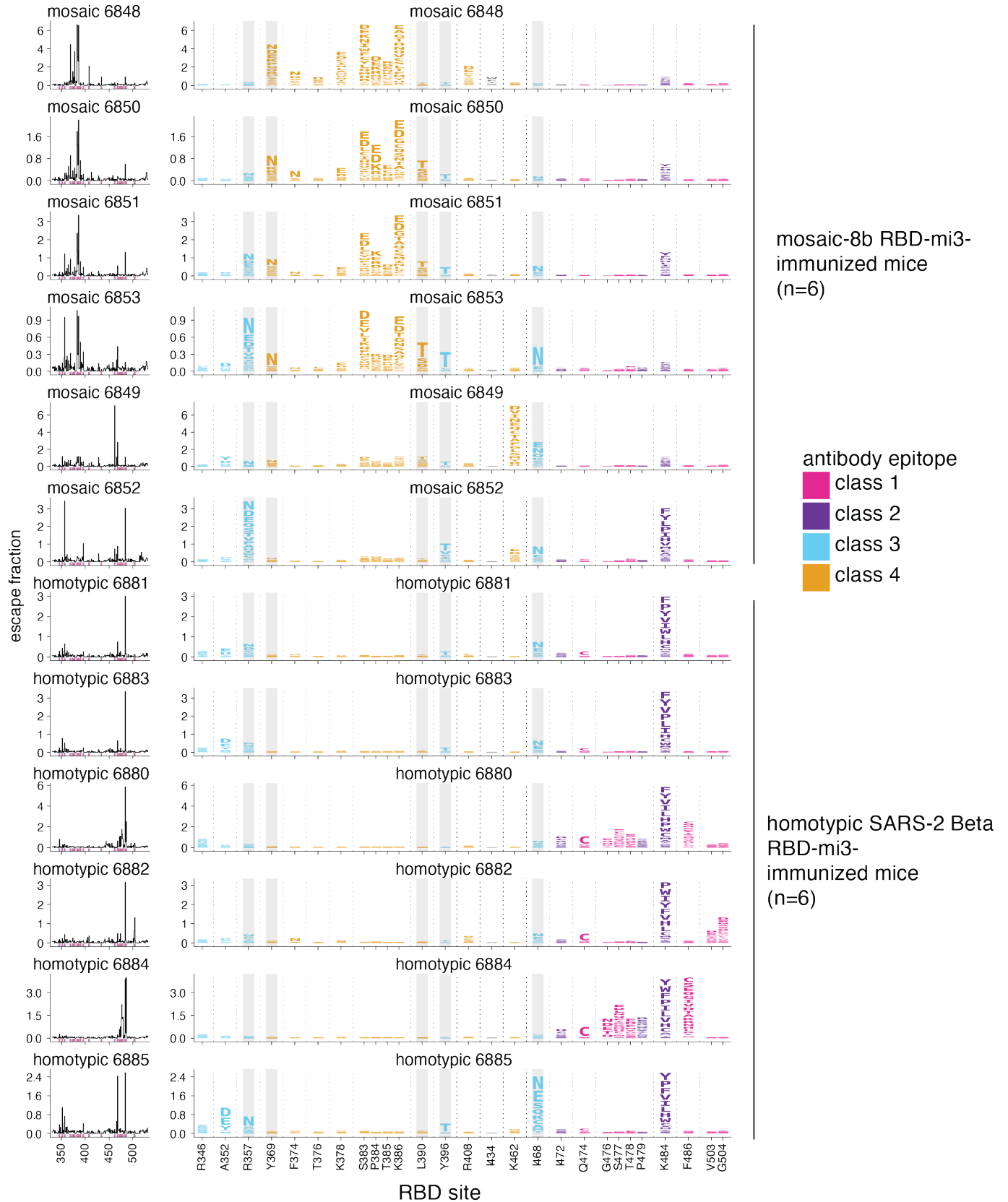
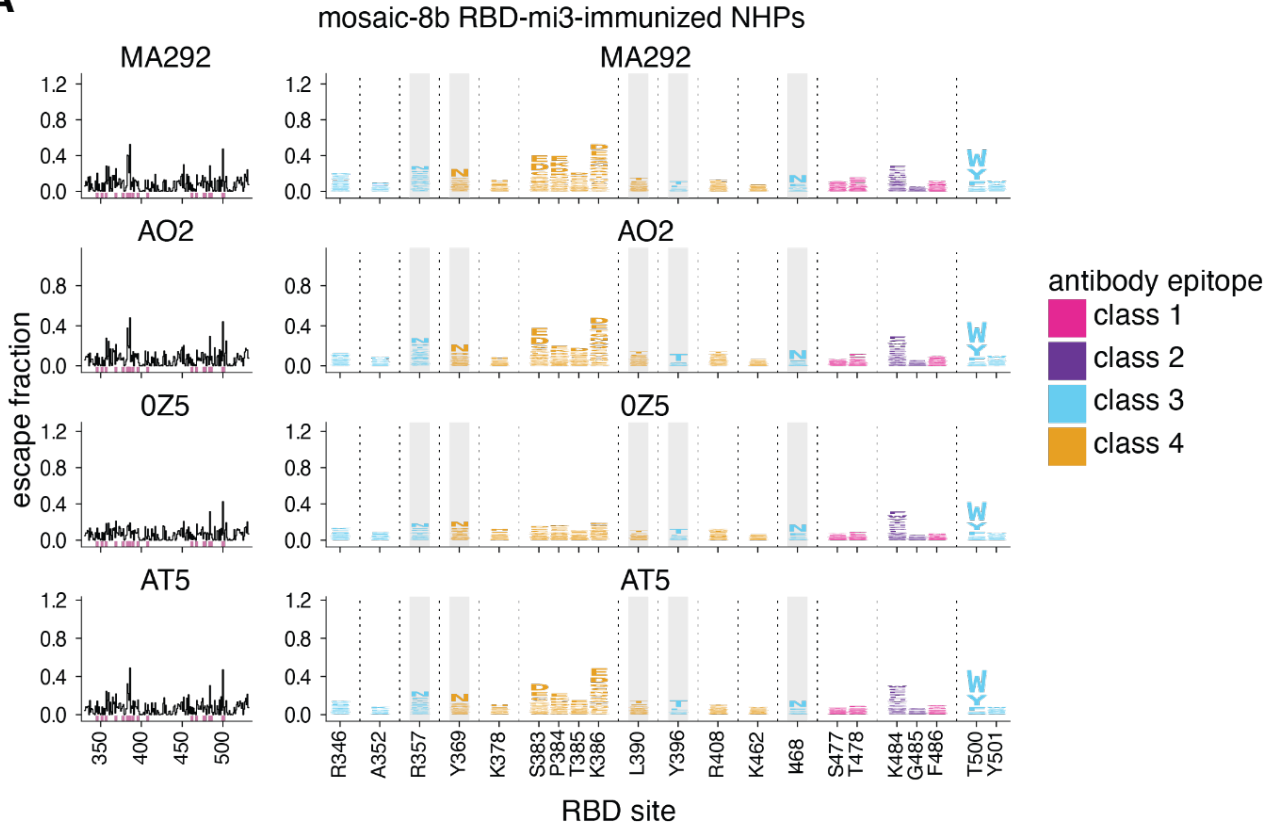
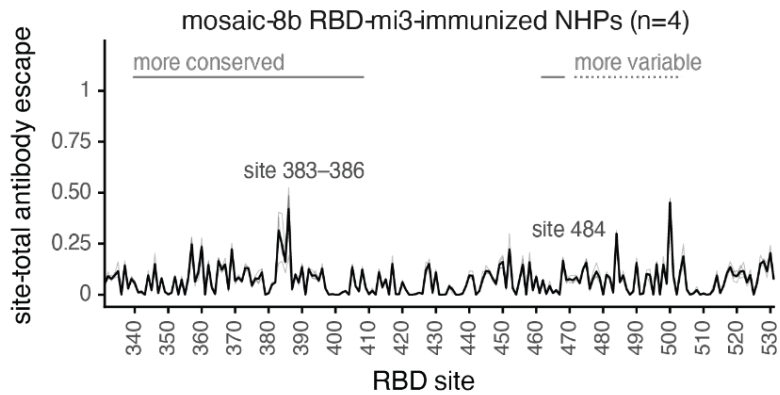


Figure S6. Complete antibody-escape maps for sera from mice immunized with the mosaic 8b-RBD-mi3 (top 6) or homotypic SARS-2 Beta RBD-mi3 (bottom 6) nanoparticles. The line plots at left indicate the sum of effects of all mutations at each RBD site on antibody binding, with larger values indicating more escape. The logo plots at right show key sites where mutations disrupted antibody binding (highlighted in purple on the line plot x-axes). The height of each letter is that mutation's escape fraction. The y-axis is scaled independently for each sample. RBD sites are colored by antibody epitope, indicated at right. Sites where some mutations introduce a potential N-linked glycosylation site sequon (NxS/T) are highlighted in gray. All escape scores are in Data S2 and at https://github.com/jbloomlab/SARS-CoV-2-RBD_Beta_mosaic_np_vaccine/blob/main/results/supp_data/all_raw_data.csv. Interactive versions of logo plots and structural visualizations are at https://jbloomlab.github.io/SARS-CoV-2-RBD_Beta_mosaic_np_vaccine/.

A



B



C

mosaic-8b RBD-mi3-immunized NHPs
site-total antibody escape, averaged across n=4 sera

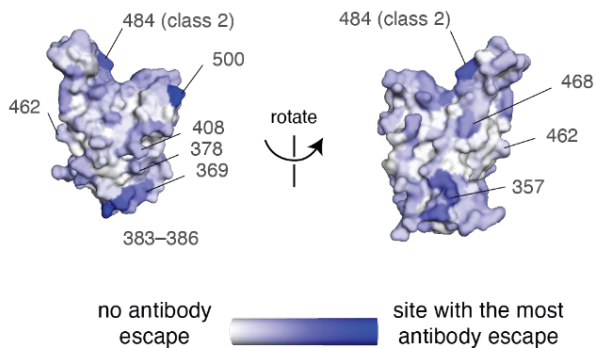


Figure S7. Complete antibody-escape maps for sera from NHPs immunized with mosaic 8b-RBD-mi3. **(A)** As in fig. S6, line plots (left) and logo plots (right) indicate the sum of the escape fractions for each mutation at a site, or mutation-level escape fractions for key sites, respectively. The y-axis is scaled independently for each sample. Sites where mutations introduce a potential N-linked glycosylation site sequon (NxS/T) are highlighted in gray. RBD sites are colored by antibody epitope, indicated in panel B. **(B)** The site-total antibody escape is averaged across n=4 sera, with the y-axis scaled as in panel A. **(C)** The average site-total antibody escape is mapped to the surface of the SARS-2 Beta RBD (PDB 7LYQ), with white indicating no escape, and blue indicating the site with the most antibody escape. Key sites are labeled, and labels are colored by antibody class. All escape scores are in Data S2 and at https://github.com/jbloomlab/SARS-CoV-2-RBD_Beta_mosaic_np_vaccine/blob/main/results/supp_data/all_raw_data.csv. Interactive versions of logo plots and structural visualizations are at https://jbloomlab.github.io/SARS-CoV-2-RBD_Beta_mosaic_np_vaccine/.

		SARS-2 Beta																			
		Lung				Mosaic-8b				Mosaic-8gm				Homotypic SARS-2 Beta				mi3 control			
H & E Staining	Lesions %	0	1	0	0	0	0	5	20	0	0	0	0	<1	30	5	0				
	Interstitial pneumonia	0	0	0	0	0	0	1	2	0	0	0	0	0	1	1	0				
	Bronchiolitis	0	1	0	0	0	0	1	2	0	0	0	0	0	1	1	0				
	perivascular leukocyte cuffing	0	0	0	0	0	0	1	2	0	0	0	1	1	3	1	0				
IHC	Staining %	0	5	0	<1	0	<1	10	40	0	<1	<1	0	<1	90	20	0				
	Type I and II pneumocytes	0	2	0	2	0	1	3	4	0	1	1	0	1	5	2	0				

		SARS-1																			
		Lung				Mosaic-8b				Mosaic-8gm				Homotypic SARS-2 Beta				mi3 control			
H & E Staining	Lesions %	0	0	0	0	0	0	<1	0	0	0	0	0	0	5	0	0				
	Interstitial pneumonia	0	0	0	0	0	0	1	0	0	0	0	0	0	1	0	0				
	Bronchiolitis	0	0	0	0	0	0	1	0	0	0	0	0	0	1	0	0				
	perivascular leukocyte cuffing	0	0	0	0	0	0	0	1	0	0	1	0	0	0	1	0				
IHC	Staining %	<1	<1	0	0	0	<1	0	0	0	0	<1	0	10	90	60	50				
	Type I and II pneumocytes	2	1	0	0	0	2	0	0	0	0	2	0	2	5	4	4				

Table S1. Pathology and immunohistochemistry (IHC) for lung tissue isolated from vaccinated K18-hACE2 mice challenged with either SARS-2 Beta or SARS-1. Scoring for hematoxylin and eosin (H&E) is as follows: 0 = not present; 1 = minimal, 1-10%; 2 = mild, 11-25%; 3 = moderate, 26-50%; 4 = marked, 51-75%; 5 = severe, 76-100%. Scoring for IHC is as follows: 0 = not present; 1 = rare/few; 2 = scattered; 3 = moderate; 4 = numerous; 5 = diffuse. Each column represents a single animal.